S©MR

СИБИРСКИЕ ЭЛЕКТРОННЫЕ
МАТЕМАТИЧЕСКИЕ ИЗВЕСТИЯ
Siberian Electronic Mathematical Reports
http://semr.math.nsc.ru
ISSN 1813-3304

*Vol. 22, No. 2, pp. 1431–1447 (2025)* УДК 519.6
https://doi.org/10.33048/semi.2025.22.088 MSC 90C25

# SECOND ORDER CONE PROGRAMMING IN CONSTRAINED PRECODING MATRIX COMPUTING FOR WIRELESS COMMUNICATION

**IRINA KOPNINA, PAVEL UYDANOV, MIKHAIL KIRICHENKO, AND VLADIMIR LYASHEV**

*Communicated by* M.A. Shishlenin

**Abstract:** A revision of the formulation on optimal criteria in digital signal processing is required upon the growing number of antennas in wireless communication systems. In particular, the advent of MIMO technology has led to the fact that the flexibility of configuring the communication system allows to adaptively control the signal strength depending on the requirements of the quality of service. The ability to change the conditions of signal transmission in wide ranges allows to redistribute power resources to more "weak" users and thereby provide a high-quality connection to a larger amount of end subscribers. To do this, it is necessary to move away from the linear problem with linear constraints (average power) to the optimization problem with quadratic constraints (taking into account the power per antenna port). In this work we give such an example and demonstrate the work of conic programming methods to solve the problem in a new formulation.

**Keywords:** massive MIMO, Quality of service, power constraint, power allocation, multi-user, beamforming.

---

Kopnina, I., Uydanov, P., Kirichenko, M., Lyashev, V., Second order cone programming in constrained precoding matrix computing for wireless communication.



*Received April, 4, 2025, Published December, 3, 2025.*

# 1 Introduction

Multiple-Input Multiple-Output (MIMO) communication networks have been considered as an effective means to enlarge system coverage and improve service coverage. There are several technologies that can be utilized for those purposes. The amplify-and-forward (AF) relay strategy is simpler to implement than other relay strategies [1]. The same time 3GPP introduced coordinated multi-point (CoMP) technique is also attractive for service coverage extension. Recently, the demand for wireless ad hoc network services, such as device-to-device (D2D) communications and internet-of-Thing (IoT) networks, has increased for their use in MIMO multi-source multidestination (MSMD) relay systems [2].

Further evolution of CoMP techniques brings to the network MIMO coordination is a very promising approach to increase signal to interference plus noise ratio (SINR) on downlinks of cellular networks without reducing the frequency reuse factor or time-frequency resource block usage. It is based on joint transmission by base stations in multi-user, multi-cell MIMO systems. The network MIMO coordinated transmission is often analyzed using a large virtual MIMO model (in some literature it is called broadcast channel model [3]). This approach increases the number of transmit antennas to each user, and the capacity increases dramatically compared to conventional MIMO networks without coordination [4]. Moreover, inter-cell scheduled transmission benefits from the increased multi-user diversity gain [5]. The capacity region of network MIMO coordination has been previously established under sum power constraint using uplink-downlink reciprocity property. However, the coordination between multiple base stations (or multiple Transmit/Receive Points, TRP) requires per-base station or even more realistic in practice per-antenna power constraints.

It is known that the capacity region is achievable with dirty paper coding (DPC). However, DPC is too complex for practical implementation. Due to their simplicity, linear precoding schemes such as multi-user zero forcing (ZF) or block diagonalization (BD) were considered [6]. However their linear constraint implementation cannot guarantee optimal solution in case of multi-TRP / multi-cell MIMO processing or shifting from maximum capacity criteria to maximum minimal SINR metric, which strictly refers to Quality of Service (QoS) measurement of the overall performance.

Another definition of multi-user precoder design is introduced in this paper. Besides this the article is introducing second-order optimization method well known in mathematics, but never used in spatial precoding algorithm design.

The article is structured in the following way: section II introduces system model, define practical methods for beamforming weight correction, describe optimal criteria as alternative to legacy one; section III is denoted to optimization problem formulation, dual problem design and second-order conic programming (SOCP) definition. Here is discussion about SOCP simplification based on application conditions. The section IV is modeling experiment description and result analysis.

## 2 SYSTEM MODEL

Considering connection on a single carrier between a base station (BS) equipped by $N_t$ transmit antennas and $N_r$ user terminals which are assumed to be equipped by a single antenna without losing the generality, a downlink precoded MIMO signal can be described as follows:

$$\mathbf{y} = \mathbf{H}\mathbf{x} + \mathbf{n}, \tag{1}$$

where $\mathbf{H} \in \mathbb{C}^{N_r \times N_t}$ - channel matrix, $\mathbf{x} \in \mathbb{C}^{N_t}$ - vector of transmission symbols, $\mathbf{y} \in \mathbb{C}^{N_r}$ - vector of received signals, and $\mathbf{n} \in \mathbb{C}\mathcal{N}(0, \sigma\mathbf{I}_{N_r})$ - complex noise vector with normal distribution, zero mean and $\sigma$ variance. In turn, the transmission vector $\mathbf{x}$ is combined from a vector of information symbols $\mathbf{s} \in \mathbb{C}^{N_r}$ weighted by matrix of spatial precoding $\mathbf{W} \in \mathbb{C}^{N_t \times N_r}$:

$$\mathbf{x} = \mathcal{P}\mathbf{W}\mathbf{s}, \tag{2}$$

where $\mathcal{P}$ - transmitting power. In order to follow the system model limitation of not exceeding the transmission power $\mathcal{P} \geq \|\mathbf{x}\|_F$ the following constraints should be applied to precoding matrix and transmitting information symbols:

$$\mathcal{P} \geq \|\mathcal{P}\mathbf{W}\mathbf{s}\|_F \geq \mathcal{P}\|\mathbf{W}\mathbf{s}\|_F,$$
$$1 \geq \|\mathbf{W}\|_F\|\mathbf{s}\|_F \geq \|\mathbf{W}\mathbf{s}\|_F$$

Thus the full radiated power system limitations can be met with the following normalization rules:

$$\|\mathbf{W}\|_F \leq 1 \tag{3}$$
$$\|\mathbf{s}\|_F \leq 1. \tag{4}$$

Assuming the information symbols $\mathbf{s}$ are corresponded to some quadrature amplitude modulation (QAM) set $\Omega$, which entities amplitude is limited by 1, then in order to follow the requirements (3) transmitting information symbols should be taken from the corresponding normalized set: $\mathbf{s} \in \{\Omega\}/\sqrt{N_r}$. For the precoder matrix $\mathbf{W}$ normalization the (3) is not the only one and the most crucial requirement is system limitation of the power emitted by each antenna of a BS leads to the constraint of transmitting signal normalization :

$$\|(\mathbf{W}\mathbf{s})_{(j)}\|_2 \leq 1/\sqrt{N_t}, j \in [1..N_t], \tag{5}$$

where $(.)_{(j)}$ means the $j$-th row of the term inside the brackets. Furthermore the (5) is consequently can be reformulated as

$$\|\mathbf{W}_{(j)}\mathbf{s}\|_2 \leq 1/\sqrt{N_t}. \tag{6}$$

Applying the property of the induced matrix norm [[7]] the (6) can be reformulated as follows:

$$\|\mathbf{W}_{(j)}\mathbf{s}\|_2 \leq \|\mathbf{W}_{(j)}\|_2\|\mathbf{s}\|_2 \leq \ 1/\sqrt{N_t}. \tag{7}$$

Since the modulation symbols amplitude is limited by 1 and every transmission layer power is mapped by equal power allocation procedure to $1/\sqrt{N_r}$ the $\|\mathbf{x}\|_2 \leq 1$. Thus the (7) converges to:

$$\|\mathbf{W}_{(j)}\| \leq \ 1/\sqrt{N_t}. \tag{8}$$

which will be considered next as *Per-Antenna Power Constraint (PAPC)* well defined in [8], [9] and [10]. In order to further compare per-antenna constraint aware precoder design approaches, beside the system efficiency metric such as bit error rate (BER) the antenna peak to average power rate (APAPR) will be considered:

$$\beta_{APAPR} = \frac{\max_i \|\mathbf{W}_{(j)}\|_2}{1/N_t \sum_i \|\mathbf{W}_{(i)}\|_2}. \tag{9}$$

Obviously as higher APAPR metric as lower energy efficiency of the overall precoder and the optimum value of $\beta_{APAPR} = 1$ As reference algorithms for PAPC satisfaction in this paper two approaches will be considered:

- *Limit-to-maximum (LTM)* approach, which normalizes all elements in $\mathbf{W}$ by maximum norm among the rows in precoding matrix scaled by antenna power limitation $\sqrt{N_t}$:

$$\mathbf{W}^{LTM} = \frac{\mathbf{W}}{\sqrt{N_t}\max_i \|\mathbf{W}_{(j)}\|_2}. \tag{10}$$

  Such normalization allow to keep the per antenna amplitude shape of every precoding and keep inter-layer interference on the same level as for original precoding $\mathbf{W}$, however the APAPR metric for LTM might reach relatively high value which means low power efficiency;
- *Limit-to-average (LTA)* approach, which normalizes every row of precoding matrix to the required per-antenna constraint, also known as equal gain transmission (EGT) [8]:

$$\mathbf{W}^{LTA}_{(j)} = \frac{\mathbf{W}_{(j)}}{\sqrt{N_t}\|\mathbf{W}_{(j)}\|_2}, \forall i. \tag{11}$$

  Easy to see the LTA approach owns the optimum value of APAPR $\beta_{APAPR} = 1$ but as the amplitude shape of the precoder vectors is changed the inter-layer interference suppression can not be granted same level as in originally computed precoder matrix $\mathbf{W}$ which might lead to significant system performance degradation.

An example of precoders amplitude shapes changes after LTA and LTM application is provided on the Fig. 1, where it can be clear seen the LTA normalization scale the power of every antenna element up to maximum allowed which makes precoder antenna amplitude shape fully distorted as compared to the original one but reaches the highest value of the APAPR (9) which means high power efficiency [10]. On the contrary, the LTM method keeps the per-antenna power shape proportionally the same with only single scale in order to make the maximum antenna power value do not exceed the limitation, but the APAPR value remains low.

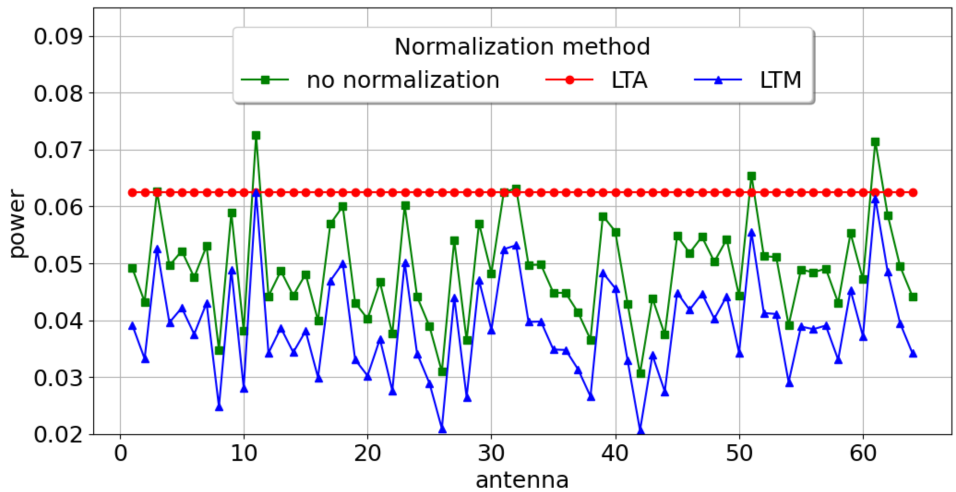


FIGURE 1. Illustration of LTM and LTA approaches

Beside the per-antenna power constraints the general target of the precoding weights computation is to maximize total UEs sum rate which is formulated as follows:

$$C = \sum_{i=1}^{N_r} B \log(1 + SINR_i), \tag{12}$$

where the $SINR_i$ describes *Signal to Interference and Noise Ratio (SINR)* of the $i$-th UE:

$$SINR_i = \frac{\mathcal{P}/N_r \|\mathbf{h}_i^H \mathbf{w}_i\|^2}{\mathcal{P}/N_r \sum_{k=1,k\neq i}^{N_r} \|\mathbf{h}_i^H \mathbf{w}_k\|^2 + \sigma^2} = \tag{13}$$

$$= \frac{\|\mathbf{h}_i^H \mathbf{w}_i\|^2}{\sum_{k=1,k\neq i}^{N_r} \|\mathbf{h}_i^H \mathbf{w}_k\|^2 + N_r\sigma^2/\mathcal{P}}$$

The QoS and resources used by a system are typically measured to assess its performance. Key metrics for this evaluation include Bit Error Rate (BER) and capacity, which are closely linked to SINRs, particularly the lowest SINR. In certain situations, it may be necessary to ensure that the SINR for each user exceeds a certain threshold value. In our model we will consider QoS constraint as

$$SINR_i \geq \gamma_i, \tag{14}$$

where the $\gamma_i$ is the required value of SINR for $i$-th UE which may be defined for example by active information transmission service requirements or MAC layer scheduler. Overall optimization goal of sum rate maximization under antenna power and QoS constraints is formulated as follows:

$$\max \sum_{i=1}^{N_r} \log B(1 + SINR_i) \tag{15}$$

$$s.t. \ \|\mathbf{W}_{(j)}\| \leq \ 1/\sqrt{N_t} \tag{16}$$

$$SINR_i \geq \gamma_i. \tag{17}$$

Historically one of the first developed precoder for linear MIMO model was an inverted channel used on transmitted site [11] named Zero-Forcing (ZF). This is a simple and efficient algorithm but it has serious defect - loss of performance for low-SNR area due to noise amplification effect. Because of this sometimes it uses in combination with matched filter (MF) - hermitian of the channel used on transmitted site. To compensate lack of the performance in different SNR areas MMSE precoder was developed [12], [13].

Another linear precoder scheme is approximate maximum-likelihood approach [14]. Also can be mentioned linear precoding technique based on decomposition [15] and nonlinear maximum likelihood [16]. There were nonlinear precoder also among which Tomilson-Harashima precoder can be mentioned [17].

One of the direction to develop new type of precoder which can satisfy several nonlinear constraints is using convex optimization methods. There were works which reformulate power maximization problem and SINR satisfaction requirements to be convex and then solve them [18], [19]. For example, in [20] considered two ways of precoder calculation: QoS constraint with power antenna minimization and maximization of SINR value with PAPC constraint which were solved using convex optimization library. The disadvantage of such reformulation is that in one task we can't guarantee SINR be more then some desired values and in another task we can't guarantee certain power level for antenna. So in our research we want to consider both QoS and PAPC constraints. In the paper [21] weighted sum rate maximization with QoS and sum-power constraint was considered, however, in practice, power amplifier of each transmit antenna has its own power budget, so it is more reasonable to consider the per-antenna power constraints. The authors in [22] used both QoS and PAPC constraints where throughput maximization was rewritten into weighted minimal mean square error(WMMSE) which was solved with ADMM method. Usually in works about optimization-based precoder calculation used optimization libraries like CVX or YALIMP. They give solution based on full-optimization scheme purposed to solve general tasks. To make solution simple, tractable and observable it is better to have custom algorithm. It is better because of: we don't need all the steps of optimization - some calculations can be omitted, some part of algorithm can be resolved analytically with simplicity. This work is devoted to develop algorithm of optimization for finding precoder using convex optimization methods which will give us custom algorithm for our problem.

## 3 OPTIMIZATION PROBLEM FORMULATION AND SOCP SOLVER

In the past few years, there has been significant advancement in the creation of effective algorithms for solving a variety of optimization problems. In order to use these algorithms, one must reformulate the problem into a standard form that the algorithms are capable dealing with. In this section we briefly introduce second order cone programming , reformulate precoder calculation into SOCP problem and an outline of the algorithm's description.

**3.1. Review of conic optimization.** SOCP is a conic program over a cone

$$K = L_{n_1} \times ... \times L_{n_N} \subset \mathbb{R}^{n_1+...+n_N} =: \mathbb{R}^n \tag{18}$$

represented as a direct product of Lorentz cones

$$L_k = \{\mathbf{x} = (x_0, x_1, ..., x_{k-1})^T \in \mathbb{R}^k | x_0 \geq \sqrt{x_1^2 + ... + x_{k-1}^2}\} \tag{19}$$

of different dimensions. In other words, a vector $\mathbf{x} \in K$ of length $n$ is composed of sub-vectors of dimensions $n_1, n_2, ..., n_N$, each of which is an element of Lorentz cone.

The program in generic form

$$\min_{\mathbf{x}\in K} \mathbf{c}^T\mathbf{x} : \mathbf{A}\mathbf{x} = \mathbf{b}, \tag{20}$$

where $\mathbf{A} \in \mathbb{R}^{m\times n}, \mathbf{b} \in \mathbb{R}^m, \mathbf{c} \in \mathbb{R}^n$ for some $m$ denoting the number of equality constraints. To problem (20) we can associate a dual problem, defined as

$$\max_{\mathbf{y},\mathbf{s}\in K^*} \mathbf{b}^T\mathbf{y} : \mathbf{s} + \mathbf{A}^T\mathbf{y} = \mathbf{c}, \tag{21}$$

Here $K^* = \{\mathbf{s}\ | \mathbf{x}^T\mathbf{s} \geq 0\ \forall \mathbf{x} \in K\}$ is dual cone to $K$, and $\mathbf{y}$ is an auxiliary real vector. The vector $\mathbf{s}$ is called the dual variable. Note that

$$\mathbf{c}^T\mathbf{x} - \mathbf{b}^T\mathbf{y} = (\mathbf{A}^T\mathbf{y} + \mathbf{s})^T\mathbf{x} - (\mathbf{A}\mathbf{x})^T\mathbf{y} = \mathbf{s}^T\mathbf{x} \geq 0 \tag{22}$$

It turns out that the optimal value for a direct problem (20) is no greater than the optimal value for a dual problem (21). Furthermore there are many conic programming methods which are applicable for the simultaneous solving primal and dual problem together in order to approach the optimal value from two sides.

**3.2. Reformulation of precoder calculation into SOCP.** The optimization of (15) with (16) and (17) is non-convex due to SINR calculation. So our approach is to find precoder matrix $\mathbf{W}$ which satisfy only optimization constraints (16) and (17) because if precoder satisfy (17) it also means that we maximize objective function (15).

The problem of finding the precoding matrix with conditions PAPC(16) , QoS(17) can be rewritten as standard SOCP problem. We will determine dimensions $n_1, n_2, ..., n_N$ defining the cone $K$ and the objects $\mathbf{A}, \mathbf{b}$ defining the equality constraints of the SOCP. There is no cost vector $\mathbf{c}$ to determine.

It turns out that conditions QoS, PAPC are equivalent to the fact that a certain set of vectors lies in Lorentz cones. The first group (16) can be written in the form

$$\|\mathbf{W}_{k*}\| = \sqrt{\sum_{l=1}^{N_t} \Re\mathbf{W}_{kl}^2 + \Im\mathbf{W}_{kl}^2} \leq 1 \xrightarrow{to\ cone} \tag{23}$$

$$\xrightarrow{to\ cone} (1, \Re\mathbf{W}_{k*}, \Im\mathbf{W}_{k*}) \in L_{2N_r+1} \tag{24}$$

Let's define $\mathbf{L} = \mathbf{HW}$ then QoS (17) condition is equivalent to

$$SINR_i \geq \gamma_i \Leftrightarrow \frac{\|\mathbf{L}_{ii}\|^2}{\sum\limits_{j=1, j\neq i}^{N_r} \|\mathbf{L}_{ij}\|^2 + \sigma^2} \geq \gamma_i \Leftrightarrow \tag{25}$$

$$\Leftrightarrow \gamma_i^{-\frac{1}{2}} \Re\mathbf{L}_{ii} \geq \sqrt{\sum_{j=1, j\neq i}^{N_r} \|\mathbf{L}_{ij}\|^2 + \sigma^2} \xrightarrow{to\ cone}$$

$$\begin{aligned}(\gamma_i^{-\frac{1}{2}} \cdot \Re\mathbf{L}_{ii}, \Re\mathbf{L}_{i1}, \Im\mathbf{L}_{i1}, .., \Re\mathbf{L}_{i,i-1}, \Im\mathbf{L}_{i,i-1},\\ \Re\mathbf{L}_{i,i+1}, \Im\mathbf{L}_{i,i+1}, .., \Re\mathbf{L}_{i,N_r}, \Im\mathbf{L}_{i,N_r}, \sigma)^T \in L_{2N_r}\end{aligned} \tag{26}$$

We get that $K = L_{2N_r+1}^{N_t} \times L_{2N_r}^{N_r}$ the direct product of $N = N_t + N_r$ Lorentz cones. The first group of $N_t$ cones $L_{2N_r+1}$ have dimension $2N_r + 1$, and the second group of $N_r$ cones has dimension $2N_r$. Then the dimension K is $n = (2N_r + 1)N_t + 2N_r^2$.

Note that not every element from the $K$ cone will satisfy the conditions (24),(26), since in the conditions (24) the first element must be equal to 1, in the conditions (26) the elements must be expressed through the matrix $\mathbf{L} = \mathbf{H}^H\mathbf{W}$. This means that certain conditions must be imposed on the cone elements in order for the conditions (24),(26) to be fulfilled. This constraints can be expressed in terms of a system of linear equations $\mathbf{Ax} = \mathbf{b}$. The equality constraints reflect links between the entries of vector $\mathbf{x} \in K$. Since the independent variables are given by entries of $\mathbf{W}$ only, the real dimension of the feasible set of the equality constraints is $2N_rN_t$. This implies are $m = n - 2N_tN_r = 2{N_r}^2 + N_t$ equations linking the elements of $\mathbf{x}$. Hence we have to construct $\mathbf{A} \in \mathbb{R}^{m\times n}, \mathbf{b} \in \mathbb{R}^m$.

The columns of $\mathbf{A}$ are associated to individual entries in the cone factors. First group of $N_t$ cones $L_{2N_r+1}$ is correspond to first $N_t(2N_r + 1)$ columns. Second group of $N_r$ cones $L_{2N_r}$ correspond to remaining $2{N_r}^2$ columns. The rows of $\mathbf{A}$ are associated to individual equations. We will show how to determine these equations which at the same time determines rows of matrix $\mathbf{A}$ and vector $\mathbf{b}$. The first $N_r$ equations is linked to cone factors

$L_{2N_r+1}$. The first entries entry is set to 1. The second group of of $N_r$ equations is linked to the second group of cone factors $L_{2N_r}$. The last entry in each of these factors is set to $\sigma$. The other equations are due to the fact that the entries of $\mathbf{W}$ appear multiple times in the description of the vector $\mathbf{x}$. These equations correspond to the fact that elements in second group are linear depend on elements from first group because $\mathbf{L} = \mathbf{H}^H\mathbf{W}$. We may express corresponding entries in the second group of the cone factors as linear function of the entries in the first group, where $\Re\mathbf{W}$ and $\Im\mathbf{W}$ using $\Re\mathbf{L}_{ij} = \sum_{k=1}^{N_t}(Re\mathbf{H}_{ki} \cdot \Re\mathbf{W}_{kj} + \Im\mathbf{H}_{ki} \cdot \Im\mathbf{W}_{kj})$ and $\Im\mathbf{L}_{ij} = \sum_{k=1}^{N_t}(\Re\mathbf{H}_{ki} \cdot \Im\mathbf{W}_{kj} - \Im\mathbf{H}_{ki} \cdot \Re\mathbf{W}_{kj})$.

So instead of solving (16) and (17) we reformulate our task into standard SOCP form

$$\mathbf{x} \in K, \mathbf{A}\mathbf{x} = \mathbf{b}, K = L_{2N_r+1}^{N_t} \times L_{2N_r}^{N_r} \tag{27}$$

For our task we can set initial point for primal and dual variables as $\mathbf{x}^0, \mathbf{s}^0, \mathbf{y}^0$ such that $\mathbf{x}^0 \in K,\ \mathbf{s}^0 + \mathbf{A}^T\mathbf{y}^0 = 0,\ \mathbf{s}^0 \in K^*$ then (27) can be rewritten into

$$\max_{\mathbf{x}\in K,\tau} \tau : \mathbf{A}\mathbf{x} = \tau\mathbf{b} + (1-\tau)\mathbf{A}\mathbf{x}^0, \tag{28}$$

If the optimal value of $\tau^*$ is at least 1, then the task (28) is achievable, otherwise it has no solution.

**3.3. Algorithm description.** There are many different methods to solve SOCP problem [23], [24] . In our paper we use one of the interior point methods [25] which solves primal and dual problem simultaneously. It helps to speed up convergence because we find optimal solution from both side. For solving primal-dual problem we will use predictor-corrector scheme where on predictor step we will update $\mathbf{x}, \mathbf{s}, \mathbf{y}, \tau$ which will increase $\tau$ value and on corrector step we change $\mathbf{x}, \mathbf{s}, \mathbf{y}$ and fix $\tau$ to improve directions for predictor step. For predictor and corrector step we need to solve system of linear equations which comes from optimal solutions for conic problem. After finding values for $\boldsymbol{\delta_x}, \boldsymbol{\delta_s}, \boldsymbol{\delta_y}$ we need to calculate step length so that new values $\mathbf{x} + \beta \cdot \boldsymbol{\delta_x}, \mathbf{s} + \beta \cdot \boldsymbol{\delta_s}$ still lies in cone.

Before going to detailed description of the algorithm, enter the necessary definitions which used in interior point method. On the interior of $L_k^o$ Lorents cone we may define the logarithmically homogeneous barrier [26]

$$F(\mathbf{x}) = -\log{(x_0^2 - x_1^2 - ... - x_k^2)} = -\log \mathbf{x}^T\mathbf{J}\mathbf{x} \tag{29}$$

where $\mathbf{J} = diag(1, -1, ..., -1) \in \mathbf{R}^{k\times k}$. Then the Hessian function of $F$ can be written

$$\mathbf{H}_\mathbf{x} = \frac{4\mathbf{J}\mathbf{x}\mathbf{x}^T\mathbf{J}^T - 2(\mathbf{x}^T\mathbf{J}\mathbf{x})\mathbf{J}}{(\mathbf{x}^T\mathbf{J}\mathbf{x})^2} \tag{30}$$

The inverse Hessian is given by

$$\mathbf{H}_\mathbf{x}^{-1} = -(\frac{\mathbf{x}^T\mathbf{J}\mathbf{x}}{2})\mathbf{J} + \mathbf{x}\mathbf{x}^\mathbf{T} \tag{31}$$

Define involution which connects primal and dual point

$$\mathbf{I}(\mathbf{x}) = -F'(x) = \frac{2\mathbf{J}\mathbf{x}}{(\mathbf{x}^T\mathbf{J}\mathbf{x})} \tag{32}$$

Inverse involution is the same as (32) but transfers dual point to primal

$$\mathbf{I^{-1}}(\mathbf{s}) = -F'(s) = \frac{2\mathbf{J}\mathbf{s}}{(\mathbf{s}^T\mathbf{J}\mathbf{s})} \tag{33}$$

Note that this definitions valid for vector in Lorents cone. The Barrier function on $K$ is given by

$$F(\mathbf{x_1}, \mathbf{x_2}, ..., \mathbf{x_k}) = \sum_{i=1}^{k} F_i(\mathbf{x_i}) \tag{34}$$

. The Hessian, the involution are computed by the corresponding formulas diagonal-block-wise or block-wise.

For interior point methods it is important to chose such initial point which lies in cone. In our case it is possible to construct initial point for dual variable $\mathbf{s}, \mathbf{y}$ and then use inverse involution find $\mathbf{x}_0 = \mathbf{I^{-1}}(\mathbf{s}_0)$. For first sub-vectors for $\mathbf{s}$ in second group set $(1, 0, , , , , 0)^T \in L_{2N_r}$

$$\mathbf{s}_{(2N_r+1)N_t+2N_r(i-1)+1} = 1, i = 1, ...N_r, \tag{35}$$

Elements in first group set

$$\mathbf{s}_{(2N_r+1)(k-1)+1+i} = -\gamma_i^{-\frac{1}{2}} \Re \mathbf{H}_{ki}$$
$$\mathbf{s}_{(2N_r+1)(k-1)+1+N_r+i} = -\gamma_i^{-\frac{1}{2}} \Im \mathbf{H}_{ki}$$
$$i = 1, ..., N_r, k = 1, ..., N_t$$

First elements in first sub-vectors should be that large that sub-vectors were inside Lorents cones.

$$\mathbf{s}_{(2N_r+1)(k-1)+1} =$$
$$1 + \|(\mathbf{s}_{(2N_r+1)(k-1)+2}, ..., \mathbf{s}_{(2N_r+1)(k-1)+1+2N_r})\| =$$
$$1 + \|diag(1/\sqrt{\gamma})\mathbf{H}_{k*}^T\|,$$

where $\mathbf{H}_{k*}$ is $k$-th row of $\mathbf{H}$ and $diag\{1/\sqrt{\gamma}\} = diag\{\sqrt{\gamma_1}, ..., \sqrt{\gamma_{N_r}}\}, k = 1, ..., N_t$ . Dual variable $\mathbf{s}$ satisfy $\mathbf{s} + \mathbf{A}^T\mathbf{y} = \mathbf{0}$ where $\mathbf{y}$ set

$$\mathbf{y}_k = -\mathbf{s}_{(2N_r+1)(k-1)+1}, k = 1, ..., N_t$$
$$\mathbf{y}_{N_t+N_r+i} = \sqrt{\gamma_i}, i = 1, ..., N_r$$

After finding dual initial variables we can construct initial point for primal variable $\mathbf{x}_0 = \mathbf{I^{-1}}(\mathbf{s}_0)$. Note that inverse involution is used for each sub-vector corresponding to Lorents cone. After setting necessary definition and initial points can write algorithm description.

**Algorithm 1** Algorithm for SOCP

**Input:** $K, \mathbf{A}, \mathbf{b}$
**Output:** $\mathbf{x} \in K : \mathbf{A}\mathbf{x} = \mathbf{b}$
$\mathbf{s} = \mathbf{s}_0, \mathbf{y} = \mathbf{y}_0, \mathbf{x} = \mathbf{x}_0$ init vectors
$\tau = 0$ {initial $\tau$}
$\xi_+ = 0.9$ - value for central path
$\theta = 0.9$ - parameter for length step
$N_{max_{iter}} = 20$ - maximum number of iterations
**while** $\tau < 1$ and $N_{iter} < N_{iter_{max}}$ **do**
  **if** $\xi(\mathbf{x}, \mathbf{s}) > \xi_+$ **then**
    $\delta_\tau = 1 - \tau$, find values $(\boldsymbol{\delta_x}, \boldsymbol{\delta_s}, \boldsymbol{\delta_y})$ for predictor step

$$\begin{bmatrix} \mathbf{0} & \mathbf{A}^T & \mathbf{I} \\ \mathbf{A} & \mathbf{0} & \mathbf{0} \\ \mathbf{I} & \mathbf{0} & \mathbf{H_x^{-1}} \end{bmatrix} \begin{bmatrix} \boldsymbol{\delta_x} \\ \boldsymbol{\delta_s} \\ \boldsymbol{\delta_y} \end{bmatrix} = \begin{bmatrix} \mathbf{0} \\ \delta_\tau(\mathbf{b} - \mathbf{A}\mathbf{x_0}) \\ -\mathbf{x} + \mathbf{I^{-1}}(\mathbf{s}) \end{bmatrix}$$

    calculate $\beta^*$ for $\mathbf{x} + \beta \cdot \boldsymbol{\delta_x}, \mathbf{s} + \beta \cdot \boldsymbol{\delta_s}$ being in cone
    $\beta = min(1, \theta \cdot \beta^*)$
    $(\mathbf{x}, \mathbf{s}, \mathbf{y}, \tau) \leftarrow (\mathbf{x}, \mathbf{s}, \mathbf{y}, \tau) + \beta(\boldsymbol{\delta_x}, \boldsymbol{\delta_s}, \boldsymbol{\delta_y}, \delta_\tau)$
    $N_{iter} = N_{iter} + 1$
  **else**
    $\delta_\tau = 0$, find values $(\boldsymbol{\delta_x}, \boldsymbol{\delta_s}, \boldsymbol{\delta_y})$ for corrector step

$$\begin{bmatrix} \mathbf{0} & \mathbf{A}^T & \mathbf{I} \\ \mathbf{A} & \mathbf{0} & \mathbf{0} \\ \mathbf{I} & \mathbf{0} & \mathbf{H_w^{-1}} \end{bmatrix} \begin{bmatrix} \boldsymbol{\delta_x} \\ \boldsymbol{\delta_s} \\ \boldsymbol{\delta_y} \end{bmatrix} = \begin{bmatrix} \mathbf{0} \\ \mathbf{0} \\ -\mathbf{x} + \mathbf{I^{-1}}(\mathbf{s}) \end{bmatrix}$$

    calculate coefficients $\beta^*$ for $\mathbf{x}, \mathbf{s}$ staying in cones
    $\beta = min(1, \beta^*)$
    $(\mathbf{x}, \mathbf{s}, \mathbf{y}) \leftarrow (\mathbf{x}, \mathbf{s}, \mathbf{y}) + \beta(\boldsymbol{\delta_x}, \boldsymbol{\delta_s}, \boldsymbol{\delta_y})$
    $N_{iter} = N_{iter} + 1$
  **end if**
**end while**
**return** $\mathbf{x}$

After finding $\mathbf{x}$ vectors then we can get precoder matrix for each $k = 1, ..., N_{tx},\ i = 1, ..., N_{ue}$ by formulas

$$Re\mathbf{W}_{ki} = \mathbf{x}_{(2N_{ue}+1)(k-1)+1+i} \tag{36}$$

$$Im\mathbf{W}_{ki} = \mathbf{x}_{(2N_{ue}+1)(k-1)+1+i+N_{ue}} \tag{37}$$

## 4 EXPERIMENTAL RESULTS and ANALYSIS

In this section, we present results of simulations for different scenarios. We compare SOCP and RZF [11] algorithms with LTA (11) and LTM (10) normalizations. As the performance evaluation metric we utilize BER. We consider an MU transmission scheme with 2 and 4 UEs. Figures Figure2, Figure3, Figure4 depicts the performance results for QPSK, QAM-16 and QAM-256 modulations. Parameters of simulation are presented in table 1.

h

| Parameters | Value | Explanation |
|---|---|---|
| TTI | 10 | Number of TTI(slot) |
| $N_{bs}$ | 1 | Number of base station(BS) |
| $N_{ue}$ | 2, 4 | Number of users(UEs) |
| $N_{rx}$ | 1 | Number of receive antennas on UE |
| $N_{tx}$ | 64 | Number of transmit antennas in BS |
| $N_{symb}$ | 14 | Number of symbols in slot |
| $RB_{size}$ | 12 | Number of RB in RBG |
| $RBG_{size}$ | 4 | Number of RBG in one TTI(slot) |
| $N_{rbgs}$ | 4 | Number rbg in simulation |
| Modulation | QPSK, QAM-16, QAM-256 | Modulation scheme |
| Channel model | 5G 3GPP - UMi | 3GPP urban micro channel model |

TABLE 1. Simulations parameters

From the Figure2 we can observe that the performance on QPSK modulation of the SOCP and RZF-LTA is similar, and the performance of RZF-LTM degrades on 2 dB for 2 UE transmission scheme and 3 dB for 4 UE transmission scheme for BER = 0.01. Obtained results can be explained by the low modulation order, which is robust to errors and interuser interference occurring after precoder per-antenna power shape distortion which together with higher transmitter power of LTA mode allows the latter to outperform the approach with the LTM normalization.

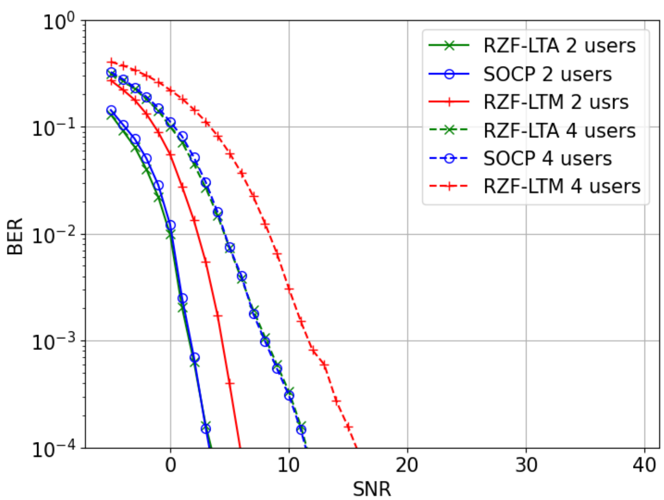


FIGURE 2. QPSK modulation

Figure3 depicts the performance for the QAM-16 modulation. On higher SNRs RZF-LTA achieves better performance than RZF-LTM. This is caused by the fact that RFZ-LTM does not introduce the interference leakage. On lower SNR range better performance of the RZF-LTA is governed by the higher transmission power. The best performance results are achieved with the proposed SOCP algorithm, which solves the direct optimization problem of satisfying QoS and PAPC constraints. Also, we can observe the plateau of BER for 4 UE transmission scheme in the considered scenario which is explained by non-ideal channel estimation and low-granularity of precoder in frequency domain: a single precoder for 48 sub-carriers corresponding to 4 resource blocks.

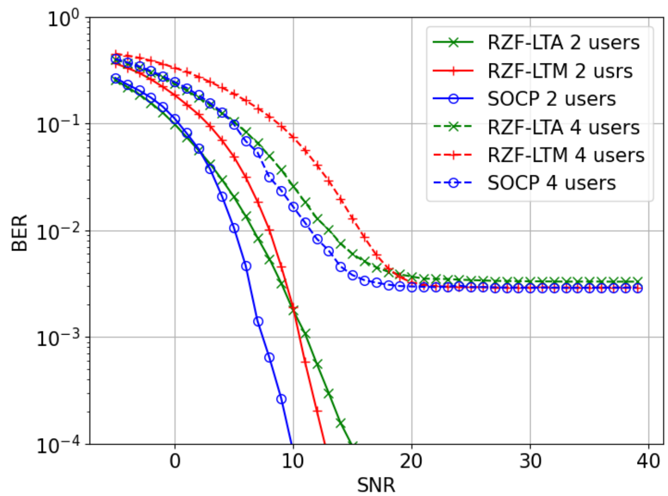


FIGURE 3. QAM-16 modulation

Figure4 provides the BER performance for QAM-256 modulation. From the obtained results we can conclude that RZF-LTA algorithm is not robust to the high-order modulations due to the interference leakage introduced on the normalization stage while more accurate RZF-LTM performs properly for 2 UEs case and out of target BER=0.01 for 4 UEs. Proposed SOCP algorithm outperforms RZF-LTM on 2 dB in 2 UEs transmission scheme which means more accurate precoder design under strict constraints of required SINR value for high order modulation. From the obtained results the following conclusions can be made. The RZF-LTM approach has good performance on lower modulation scheme. After LTM normalization RZF has interference leakage so it is better to use RZF-LTA on higher modulations. SOCP solution showed performance gain from 2 to 4 db comparing to RZF-LTM and RZF-LTA depending on different scenarios. It happens because SOCP solves direct optimizes task of satisfying QoS and PAPC constraint simultaneously.

As the evidence of SOCP-based approach high power efficiency the averaged APAPR distribution among SINR is shown on the Fig.5: it is clear to see the behaviour of SOCP approach is closer to LTA mode ($\beta_{APAPR} = 1$)

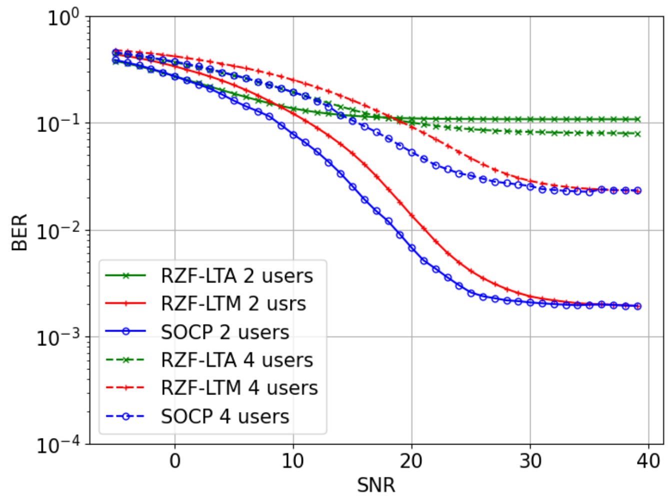


FIGURE 4. QAM-256 modulation

in low and medium SINR region where the transmitting power is more important than keeping precoder antenna power shape due to robust to errors and interference low order modulation is in use, while in high SINR region SOCP approach adopts to strong requirements of SINR for high order modulation and behave similar to LTM mode enlarging APAPR but carefully suppressing the inter-user interference.

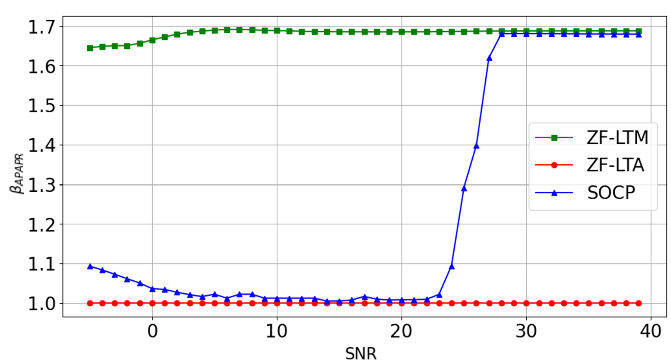


FIGURE 5. $\beta_{APAPR}$ calculation for different precoder methods

## 5 Application discussion

Today, 5.5G is already on the road, and new use cases have been introduced that combine features of the original 5G use cases; (i) uplink centric broadband communication (UCBC) which refers to massive things with broadband abilities such as HD video uploading and machine vision; (ii) real-time broadband communication (RTBC), which combines broadband features with high reliability such as extended reality applications and holograms; (iii) integrated sensing and communications (ISAC) which integrates both communications and sensing capabilities in applications like positioning, spectroscopy, and imaging.

Owing to this, it is difficult to predict exactly what 6G will be, but the research community seems to agree that 6G will be the seed for enabling extremely immersive experiences, haptics, industry 4.0 with connected intelligence, 3D full coverage of the earth, and native artificial intelligence (AI)-empowered wireless communication. Furthermore, fog computing enjoys several advantages that can be leveraged to complement edge and cloud computing in 6G [27]. All these aspects of further network evolution have strong requirements to the QoS metrics. Maybe there is no maximal capacity request, but clear minimal guarantee SINR that makes SOCP tool more and more attractive for new immersive scenarios.

Also latency factor becomes important in industry 4.0. Thus delay-bounded QoS was introduced in [28]. Due to the time-varying wireless channels, the deterministic delay-bounded QoS requirements are difficult to achieve. Therefore, the alternative statistical delay-bounded QoS provisioning theory has been proposed to be a useful technique to provide the delay-bounded QoS [28] guarantee for real-time wireless traffic. This also potential embeding point for SOCP tool to support deterministic delay-bounded QoS requirements.

## 6 Conclusion

This paper introduces a novel approach to precoder design using SOCP, which takes into account SINR limitations and PAPC. The results demonstrate that the SOCP-based approach is highly adaptable and outperforms other normalization methods such as LTA and LTM. Specifically, the SOCP approach achieves maximum power utilization in low SINR regions with robust modulation schemes, while maintaining the antenna power shape with high APAPR in high SINR regions with sensitive high order modulation schemes. Furthermore, the SOCP method is shown to be highly efficient as it does not require any approximation of quadratic constraints, unlike linear and quadratic programming methods.

## References

[1] O. Munoz-Medina, J. Vidal, A. Agustin, *Linear transceiver design in nonregenerative relays with channel state information*, IEEE Trans. Signal Process., **55**:6 2007, 2593–2604. Zbl 1391.94689

[2] H.-J. Choi, C. Song, H. Park, I. Lee, *Transceiver designs for multipoint-to-multipoint MIMO amplify-and-forward relaying systems*, IEEE Trans. Wireless Commun., **13**:1 (2014), 198–209.

[3] A. Goldsmith, S.A. Jafar, N. Jindal, S. Vishwanath, *Capacity limits of MIMO channels*, IEEE J. Selected Areas Commun., **21**:5 (2003), 684–702.

[4] O. Somekh, B.M. Zaidel, S. Shamai, *Sum rate characterization of joint multiple cell-site processing*, IEEE Trans. Inform. Theory, **53**:12 (2007), 4473–4497.

[5] Wan Choi, J.G. Andrews, *The capacity gain from intercell scheduling in multi-antenna systems*, IEEE Trans. Wireless Commun., **7**:2 (2008), 714–725.

[6] Q.H. Spencer, A.L. Swindlehurst, M. Haardt, *Zero-forcing methods for downlink spatial multiplexing in multiuser MIMO channels*, IEEE Trans. Signal Process., **52**:2 (2004), 461–471. Zbl 1369.94294

[7] C.D. Meyer, *Matrix analysis and applied linear algebra*, Society for Industrial and Applied Mathematics, Philadelphia, 2000. Zbl 0962.15001

[8] S. Zhang, R. Zhang, T.J. Lim, *Massive MIMO with per-antenna power constraint*, In *2014 IEEE Global Conference on Signal and Information Processing (GlobalSIP)*, 2014, 642–646.

[9] S. Kaviani, W.A. Krzymien, *Optimal multiuser zero forcing with per-antenna power constraints for network MIMO coordination*, EURASIP J. Wirel. Commun. Netw., **2011**:1 (2011), Paper No. 190461.

[10] H. Jedda, A. Mezghani, A.L. Swindlehurst, J.A. Nossek, *Precoding under instantaneous per-antenna peak power constraint*, in 2017 25th European Signal Processing Conference (EUSIPCO), 863–867, 2017.

[11] B.R. Vojčić, W.M. Jang, *Transmitter precoding in synchronous multiuser communications*, IEEE Trans. Commun., **46**:10 (1998), 1346–1355.

[12] R.L.-U Choi, R.D. Murch, *New transmit schemes and simplified receivers for MIMO wireless communication systems*, IEEE Trans. Wireless Commun., **2**:6 (2003), 1217–1230.

[13] L.-U Choi, R.D. Murch, *Transmit-preprocessing techniques with simplified receivers for the downlink of MISO TDD-CDMA systems*, IEEE Trans. Vehicular Technol., **53**:2 (2004), 285–295.

[14] S. Wang, J. Caffery, H. Shen, *Linear multiuser precoding for synchronous CDMA*, 2003 IEEE Wireless Communications and Networking, vol.1, 2003 403–407.

[15] L.-U Choi, R.D. Murch, *A transmit preprocessing technique for multiuser MIMO systems using a decomposition approach*, IEEE Trans. Wireless Commun., **3**:1 (2004), 20–24.

[16] L. Collin, O. Berder, P. Rostaing, G. Burel, *Optimal minimum distance-based precoder for MIMO spatial multiplexing systems*, IEEE Trans. Process., **52**:3 (2004), 617–627. Zbl 1369.94120

[17] R.D. Wesel, J.M. Cioffi, *Achievable rates for Tomlinson-Harashima precoding*, IEEE Trans. Inf. Theory, **44**:2 (1998), 824–831. Zbl 0910.94014

[18] Zhi-Quan Luo, Wei Yu, *An introduction to convex optimization for communications and signal processing*, IEEE J. Selected Areas Commun., **24**:8 (2006), 1426–1438.

[19] M.B. Shenouda, T.N. Davidson, *Convex conic formulations of robust downlink precoder designs with quality of service constraints*, IEEE J. Selected Topics Signal Process., **1**:4 (2007), 714–724.

[20] A. Wiesel, Y.C. Eldar, S. Shamai, *Linear precoding via conic optimization for fixed MIMO receivers*, IEEE Trans. Signal Process., **54**:1 (2006), 161–176. Zbl 1373.94731

[21] Ting Ma, Qingjiang Shi, Enbin Song, *QoS-constrained weighted sum-rate maximization in multi-cell multi-user MIMO systems: An admm approach*, 2016 35th Chinese Control Conference (CCC), 6905–6910, 2016.

[22] Kaiyi Chi, Yingzhi Huang, Qianqian Yang, Zhaohui Yang, Zhaoyang Zhang, *MIMO precoding design with QoS and per-antenna power constraints*, GLOBECOM 2023 - 2023 IEEE Global Communications Conference, 3324–3329, 2023.

[23] Zhi Cai, Kim-Chuan Toh, *Solving second order cone programming via a reduced augmented system approach*, SIAM J. Optim., **17**:3 (2006), 711–737, 09 2006. Zbl 1128.90045

[24] Y. Nesterov, A. Nemirovskii, *Interior-point polynomial algorithms in convex programming*, SIAM Studies in Applied Mathematics, **13**, SIAM, Philadelphia, 1994. Zbl 0824.90112

[25] S.J. Wright, *Primal-dual interior-point methods*. Society for Industrial and Applied Mathematics, Philadelphia, 1997. Zbl 0863.65031

[26] Yu. Nesterov, M. Todd, *Self-scaled barriers and interior-point methods for convex programming*, Mathematics of Operations Research – MOR, **22**:1 (1997), 1–42.

[27] M. Chafii, L. Bariah, S. Muhaidat, M. Debbah, *Twelve scientific challenges for 6g: Rethinking the foundations of communications theory*, IEEE Commun. Surveys & Tutorials, **25**:2 (2023), 868–904.

[28] Xi Zhang, Qixuan Zhu, H.V. Poor, *Heterogeneous statistical qos provisioning for scalable software-defined 6g mobile networks*, 2023 57th Annual Conference on Information Sciences and Systems (CISS), 1–6, 2023.

Irina Kopnina
Institute of Numerical Mathematics, Russian Academy of Sciences
8 Gubkina Street
Moscow City
Moscow
119333, Russia
*Email address*: kopnina_i@mail.ru

Pavel Uydanov
Moscow Radio Transmission Technology Lab.
1 Lenin Hills, building 75b
Moscow City
Moscow
119234, Moscow, Russia
*Email address*: uydanov@rtt-lab.ru

Mikhail Kirichenko
Moscow Radio Transmission Technology Lab.
1 Lenin Hills, building 75b
Moscow City
Moscow
119234, Moscow, Russia
*Email address*: kirichenko@rtt-lab.ru

Vladimir Lyashev
Moscow Institute of Physics and Technology,
9 Institutskiy Lane
Dolgoprudny City
Moskovskaya oblast
141700, Moscow, Russia
*Email address*: lyashev.va@mipt.ru